

# CHAPTER 5

## EXPERIMENTAL DETAILS

### I. MEASUREMENT ELECTRONICS

#### 5.1 A.C. Measurement of Conductance

As described in section 3.2, the most direct way of investigating a superconductor's density of excitation states is to measure the bias-dependent dynamic conductance,  $dI(V)/dV$ , of an SIN junction. A standard technique for measuring this quantity is to apply to the sample a d.c. bias,  $V_0$ , on which is superimposed a small sinusoidal modulation of angular frequency  $\omega$  and r.m.s. amplitude  $\delta V$ . The current flowing through the sample will contain a component of frequency  $\omega$ , which is proportional to

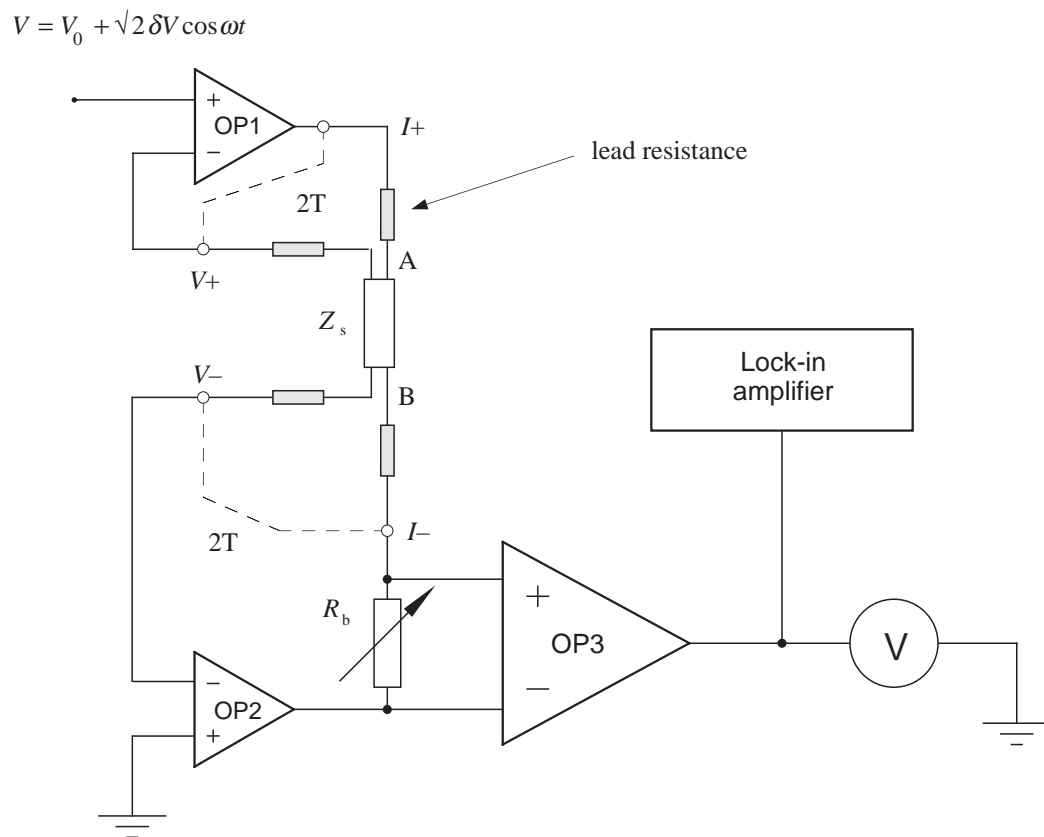


**Fig. 5.1.** Schematic diagram of the circuit used to measure conductance–voltage characteristics. The sample is represented by impedance  $Z_s$ . Practical design details of this circuit are discussed in appendix A.

$dI(V_0)/dV$  and may be detected with a phase sensitive detector (PSD, or equivalently ‘lock-in amplifier’). Sweeping the d.c. bias whilst recording the PSD output yields the sample’s conductance–voltage characteristic. A non-ohmic sample will also produce harmonics of this fundamental frequency from which the higher-order derivatives may be found. The design of spectrometers using this a.c. modulation technique is reviewed by Wolf (1985, p.505). In this study the sample conductance was measured using an active voltage-biasing spectrometer (figure 5.1), based on a design by Edgar (1987).

The modulation voltage and d.c. bias were combined by an audio-frequency transformer. The resulting signal,  $V_0 + \sqrt{2} \delta V \cos \omega t$ , was applied to the non-inverting input of an op-amp (OP1) which held one side (A) of the sample at this voltage, independent of sample or lead resistances. The other side (B) of the sample was maintained at the circuit’s ground potential by a similar op-amp loop (OP2). Voltage biasing the sample ensures that the modulation amplitude is constant and results in a simple relationship between the output of the PSD and the dynamic conductance.

Op-amps with extremely low input bias currents ( $< 10$  pA) were used so that when operating in four-terminal mode (with the ‘2T’ links removed) all current flowing through the sample,  $Z_s$ , passed through the sensing resistor,  $R_b$ . This current may be expressed as a Taylor series expansion about the d.c. bias,  $V_0$ :

$$\begin{aligned}
 I(V) &= I(V_0) + \left( \frac{dI}{dV} \right)_{V_0} \sqrt{2} \delta V \cos \omega t + \frac{1}{2!} \left( \frac{d^2 I}{dV^2} \right)_{V_0} (\sqrt{2} \delta V \cos \omega t)^2 + O(\delta V^3) \\
 &\approx I(V_0) + \left( \frac{dI}{dV} \right)_{V_0} \sqrt{2} \delta V \cos \omega t + \frac{1}{2} \left( \frac{d^2 I}{dV^2} \right)_{V_0} \delta V^2 \cos 2\omega t
 \end{aligned} \tag{5.1}$$

The voltage drop across  $R_b$  was amplified by an instrumentation amplifier (OP3) with gain  $A$  and input to both a voltmeter and a lock-in amplifier. These measure a voltage proportional to each term in the series expansion and so allow the current and derivatives to be calculated from

$$I(V_0) = V_{dc} / R_b A \tag{5.2}$$

$$\left( \frac{dI}{dV} \right)_{V_0} = \frac{V_{\omega}(V_0)}{\delta V R_b A} \tag{5.3}$$

$$\left( \frac{d^2 I}{dV^2} \right)_{V_0} = \frac{2\sqrt{2} V_{2\omega}(V_0)}{\delta V^2 R_b A} \tag{5.4}$$

where  $V_{dc}$  is the voltmeter reading and  $V_{\omega}$  and  $V_{2\omega}$  are the r.m.s. fundamental and second-harmonic voltages measured by the lock-in. If the sample is purely resistive then (5.3) and (5.4) are the dynamic conductance and its derivative respectively, and the PSD is simply used to measure the amplitude of the input signal. If the sample has some capacitance then the total current is

$$I(V) = I_{dc}(V) + C(V) \frac{dV}{dt}$$

where  $C$  is the sample's dynamic capacitance,  $dq/dV$ , and  $dV/dt = \omega\sqrt{2}\delta V \sin \omega t$ . The dynamic conductance,  $G$ , is  $dI_{dc}/dV$  so

$$\frac{dI}{dV} = G(V) + C'(V) \frac{dV}{dt}$$

and

$$\frac{d^2I}{dV^2} = G'(V) + C''(V) \frac{dV}{dt}$$

Substituting these into (5.1) gives expressions for the dynamic conductance and capacitance and their derivatives, in terms of the in-phase ( $V^{\parallel}$ ) and quadrature ( $V^{\perp}$ ) voltages measured by the lock-in amplifier,

$$G(V_0) = \frac{V_{\omega}^{\parallel}(V_0)}{\delta V R_b A} \quad \text{and} \quad C(V_0) = \frac{V_{\omega}^{\perp}(V_0)}{\delta V R_b A \omega}$$

$$\left(\frac{dG}{dV}\right)_{V_0} = \frac{2\sqrt{2} V_{2\omega}^{\parallel}(V_0)}{\delta V^2 R_b A} \quad \text{and} \quad \left(\frac{dC}{dV}\right)_{V_0} = \frac{\sqrt{2} V_{2\omega}^{\perp}(V_0)}{\delta V^2 R_b A \omega}$$

The phase is with respect to the voltage across the sample so this information must be supplied to the lock-in amplifier. This was done by adjusting the phase control to zero the quadrature voltage measured at the input to OP1\*. The in-phase voltage was then  $\delta V$ .

The d.c. bias was provided by a function generator and input to both OP1 and the x-axis of a chart recorder. The y-axis of the chart recorder was connected to either the OP3 output, to measure current, or the PSD output to measure  $dI(V)/dV$  or  $d^2I(V)/dV^2$ . The recorded traces were later digitised and calibrated. The modulation was supplied by the internal oscillator of the lock-in amplifier (EG&G PAR model

---

\* This method will not work if the op-amps or differential amplifier introduce a phase shift or attenuate the modulation signal. See appendix A.

5210) or by a Krohn-Hite 4400A oscillator. A modulation frequency of about 1 kHz was used, this being well within the bandwidth of the op-amps and a compromise between reducing sample  $1/f$  noise, reducing noise in the electronics (increasing with frequency) and reducing the capacitive current. Harmonics of the mains frequency (50 Hz) were avoided. The modulation amplitude was chosen to reduce the instrumentation broadening inherent in the modulation technique (see appendix A) to the same level as thermal broadening, (i.e., for measurements of elastic tunnelling conductance,  $\sqrt{3} \delta V < 3.52 k_B T$ ). Reducing the modulation amplitude decreases the signal-to-noise ratio and so requires a longer lock-in time constant and hence a longer measurement time.

Care must be taken to ensure that the sample leads are properly connected to all four terminals of the sample. A break in one of the leads will open a feedback loop causing the op-amp's output to saturate at 15 V, possibly damaging the junction\*. To guard against this the feedback loops were initially kept closed by switchable links (illustrated by the dashed lines labelled '2T'), which allowed the circuit to make two-terminal measurements. Before opening the links the condition of the sample leads and contacts was monitored by measuring an  $I(V)$  curve with only two of the leads connected (e.g.,  $I+$  and  $I-$ ); clearly if any current was observed the leads and contacts were continuous. This was repeated for the other pair of leads. Usually the lead resistance was much smaller than the sample resistance and there was very little difference between characteristics obtained in the two-terminal and four-terminal configurations.

### 5.1.1 Conductance-Bridge Measurements

The circuit shown in figure 5.1 was used to measure samples in which the conductance changed significantly over the bias range of interest. Many junctions made in the early stages of this study had much more linear  $I-V$  characteristics in which the conductance changed by only a few percent. To improve the accuracy of measurements on such junctions the voltage-biasing electronics was incorporated into a conductance bridge (figure 5.2).

When the bridge is balanced by a parallel resistor and capacitor ( $R_b$  and  $C_b$ ) the sample conductance and capacitance are given by<sup>†</sup>

---

\* To ensure that the lower feedback loop remains closed, switches used to select the value of  $R_b$  must be 'make before break'.

<sup>†</sup> A derivation of the calibration equations and an analysis of errors can be found in the thesis of Speakman (1992, ch.3).

and

$$G(V) = G(V_b) \left[ 1 - \frac{\beta}{\delta V} (V_{\omega}^{\parallel}(V) - R_b C_b \omega V_{\omega}^{\perp}(V)) \right] \quad (5.5)$$

$$C(V) = C(V_b) \left[ 1 - \frac{\beta}{\delta V} \left( V_{\omega}^{\parallel}(V) + \frac{V_{\omega}^{\perp}(V)}{R_b C_b \omega} \right) \right]$$

where  $\beta = 1 + \kappa$ ,  $\kappa = R_3/R_4$  and the conductance and capacitance at balance are

$$G(V_b) = 1/\kappa R_b \quad \text{and} \quad C(V_b) = C_b/\kappa$$

The capacitance and conductance derivatives can also be found from the second-harmonic signal. Most superconducting tunnel junctions have a negligible (and unimportant) capacitance so balance was achieved using just a resistor ( $C_b = 0$ ). In this case

$$G(V) = G(V_b) \left[ 1 - \frac{\beta}{\delta V} V_{\omega}^{\parallel}(V) \right] \quad (5.6)$$

and

$$C(V) = -G(V_b) \left[ \frac{\beta}{\delta V \omega} V_{\omega}^{\perp}(V) \right]$$

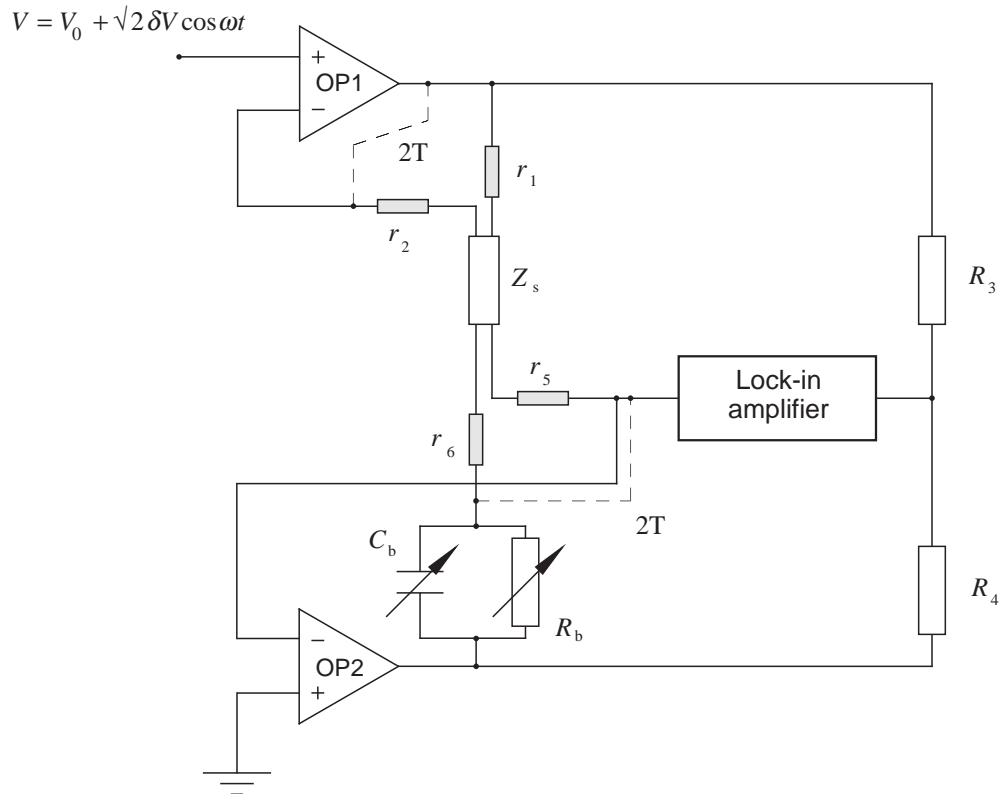


**Fig. 5.2.** Schematics of the conductance bridge used to measure junction characteristics.

In the bridge configuration the lock-in amplifier output is proportional to the conductance change from the balance condition, so the dynamic range is increased and changes of less than 1% may be detected. An additional advantage of the bridge configuration is that noise generated in the voltage source appears across both arms of the bridge and does not affect the lock-in, which measures the difference signal.

## 5.2 D.C. Measurement of Conductance

The a.c. modulation method was very convenient for measurement of the conductance of stable tunnel junctions. An analogue voltage source could be swept slowly through the bias range of interest and the output of the lock-in amplifier recorded on a chart recorder. Noise in the measured conductance was reduced to acceptable levels simply by raising the lock-in's time constant and sweeping more slowly. Typically a single conductance curve would take several minutes to collect.

This was not a practical method, however, for measuring the conductance–voltage characteristics of vibration-sensitive point-contact junctions; a particular  $I$ – $V$  characteristic would remain stable for several minutes and then change unpredictably. Initially the experimental procedure was to sweep the sample bias using a 30 Hz triangular waveform and monitor the  $I$ – $V$  curve of the contact on an oscilloscope whilst manipulating the point. When interesting characteristics were obtained the sensitivity of the lock-in amplifier was set to an appropriate level and a slow sweep to measure the conductance–voltage curve was started. On most attempts good data would be collected from only part of the voltage range of interest and then the junction would be disturbed resulting in a dramatic jump in the lock-in amplifier's output.

It would be better to obtain data from the full bias range of interest even if signal-to-noise ratio was compromised to achieve this. A large amount of potentially useful data-acquisition time was also wasted in setting up the lock-in amplifier, replacing chart-recorder paper and placing calibration marks on the recorded trace.

To solve these problems the d.c.  $I$ – $V$  characteristics of point-contact junctions were measured using a computer-controlled data-acquisition system, designed and built by the author. This consisted of a digital-to-analogue converter (DAC) generating a voltage ramp which was input to OP1 in figure 5.1, and an analogue-to-digital converter (ADC) recording the instrumentation amplifier's output voltage (i.e., the current signal). The lock-in amplifier was not used and the differential conductance was found by numerical differentiation of the  $I$ – $V$  curve.

The DAC and ADC were part of a CIL6580 data-acquisition unit\*. This also incorpo-

---

\* Manufactured by CIL Microsystems, Lancing, Sussex.

rated variable-gain differential amplifiers, digital filtering, an RS-232 (or optionally an IEEE-488) interface and a low-level programming language. The DAC and ADC were 16 bit and digitisation noise was not found to be a problem.

The CIL6580 unit was controlled by a host computer<sup>†</sup> running a custom-written Pascal program. This allowed the user to define a table of voltages, which would be output sequentially by the DAC to the sample-biasing electronics. For each element in the table the program output the required voltage, waited for a user-defined period of time, then measured the output of the instrumentation amplifier. In this way the  $I-V$  curve for the sample was measured point by point and displayed by the computer, which effectively acted as an oscilloscope. Whilst monitoring the display the point contact was adjusted and, when interesting characteristics were obtained, data acquisition could be started simply by pressing a button. No time was wasted in preparing the chart recorder and useful data was collected from even the most transient of contacts. On completing a voltage sweep the recorded  $I-V$  points were saved in a simple ASCII format data file, which could later be read by a number of custom-written and standard data-processing packages. The spectrometer control program was optimised for rapid data gathering with minimum loss of data-acquisition time due to setting measurement parameters etc.

### 5.2.1 Calibration of Raw Data

Computer control also allowed the data to be digitised and calibrated automatically. This was done laboriously by hand for curves previously recorded on paper by a chart recorder. The calibration models are schematically illustrated in figure 5.3.

$V_{\text{nom}}$  is the voltage defined by the user in the look-up table and  $N$  is the 16-bit number output by the ADC. These are the two items of raw data ‘known’ by the computer and input to the calibration routines of the program.  $AF$  is the attenuation factor of a potential divider used to reduce the  $\pm 10$  V output of the DAC to the required sample voltage.

The gain and offset parameters of the DAC and ADCs were found by fitting a straight line to 50 output and input voltages measured with a Thurlby 1905a multimeter. Using these linear calibration models the CIL6502 unit was capable of measuring and outputting voltages with an error of less than 0.1%. After six months these calibration parameters were rechecked and found to be identical to within 0.05%.

The sensing resistors,  $R_{\text{sense}}$  ( $R_b$  in figure 5.1), which ranged from  $2 \Omega$  to  $20 \text{ M}\Omega$ , were measured with an error of less than 0.4%, also with the Thurlby 1905a multimeter.

---

<sup>†</sup> Apple Macintosh Plus, 2 MHz 68000 processor, 2 Mb memory, 40 Mb hard disk.

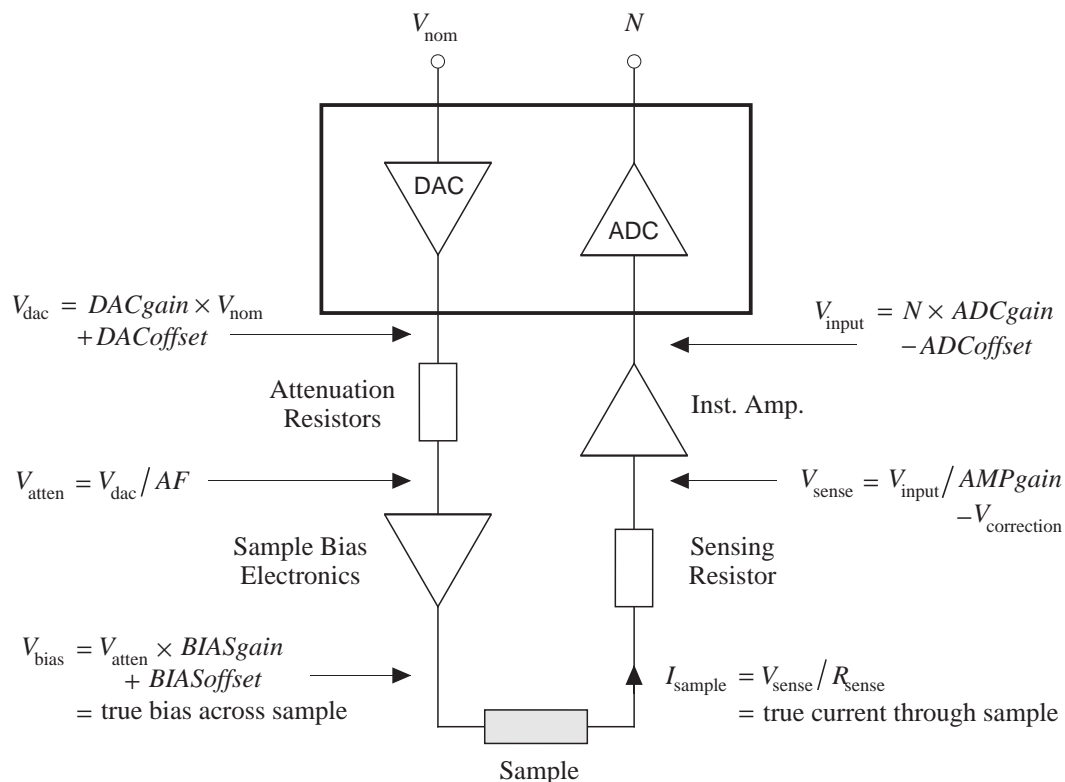


**Fig. 5.3.** Calibration of the measurement system.  $V_{nom}$  and  $N$  are the quantities 'known' by the computer. Currents and voltages at other points in the system can be calculated from these via the linear calibration models defined here.

The calibration parameters of other elements in the measurement system (i.e.,  $AF$ ,  $BIASgain$ ,  $BIASoffset$ ,  $AMPgain$ ) were found by using the CIL6580 unit (plus calibration models for its DAC and ADCs) to apply a voltage to the element and to measure its response. Several hundred voltages could be output and the parameters found by fitting a straight line. The d.c. gain of the sample-biasing electronics was always unity and the instrumentation-amplifier gain was exactly the value expected from its circuit-board connections. In addition, the instrumentation amplifier's offset was trimmed on the circuit board to negligible levels and was not included in the calibration models\*.

Because the calibration parameters were expected to change (either through modification of the circuitry or by long-term drift) they were stored in the 'resource fork' of the program and read into memory when the program was first launched. They could be changed with a resource editor (e.g., ResEdit, Apple Computer, Inc.) and modification of source code was unnecessary. One parameter,  $V_{correction}$ , could be set whilst the program was running. No current can be flowing when the tip is retracted from the sample so any voltage measured at the ADC input must arise through

\* Any error in this assumption could be accommodated by the run-time offset correction,  $V_{correction}$ .

an instrumentation-amplifier offset or through thermoelectrically induced voltages. A routine in the program allowed this stray voltage to be measured and subsequently subtracted from all following measurements.

There were three principal sources of error in the calibrated data - noise and residual offset in the electronics and errors in the calibration model. The  $I$ - $V$  characteristics of known resistances were measured and analysed to determine empirically the total error appearing in the current and the numerically calculated conductance. Acquisition and processing of this dummy data was done in exactly the same way as for real data. The results of these tests are summarised in figures 5.4–6. The position of conductance peaks in the tunnelling characteristics of conventional SIS tunnel junctions indicated that residual offset in the sample bias was smaller than 0.05 mV. Sources of noise and calibration errors are discussed in appendix A.

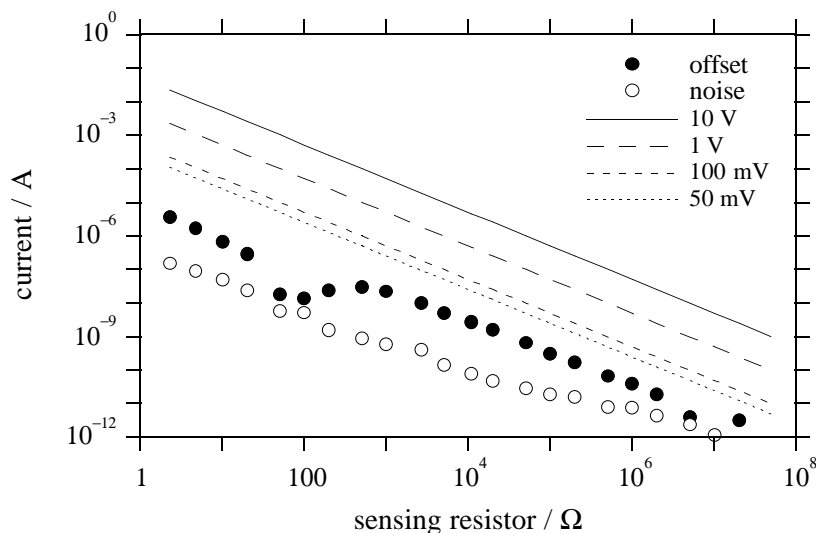


**Fig. 5.4.** Noise and offset in current for each value of the sensing resistor. Measurements were made by taking 101 readings of current with ADC range set to 100 mV and no sample connected. The offset was taken from the mean of these readings and the noise from the standard deviation. Lines show full-scale current for each ADC range. In these measurements the run-time offset correction,  $V_{\text{correction}}$ , was not used, so this data shows the raw, worst-case offset.

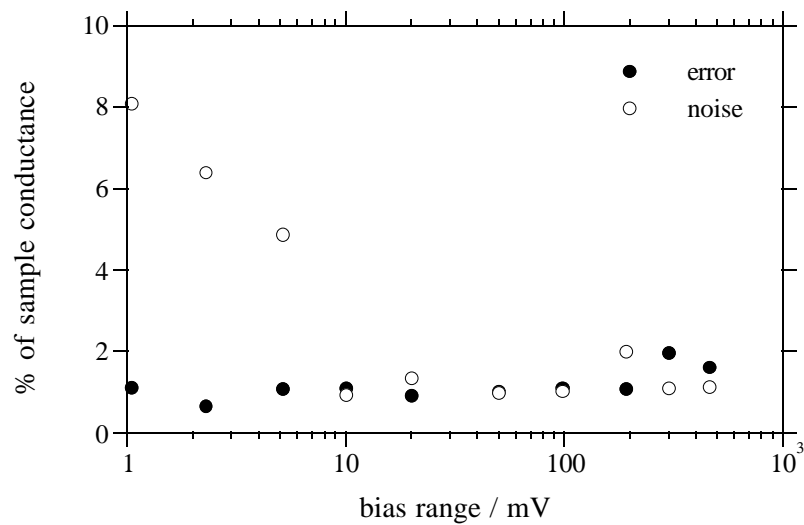


**Fig. 5.5.** Error and noise in the numerically calculated conductance of a 1 M $\Omega$  dummy sample. The conductance was calculated from  $I$ - $V$  characteristics measured over a range of bias voltages - each sweep containing 101  $I(V)$  points.

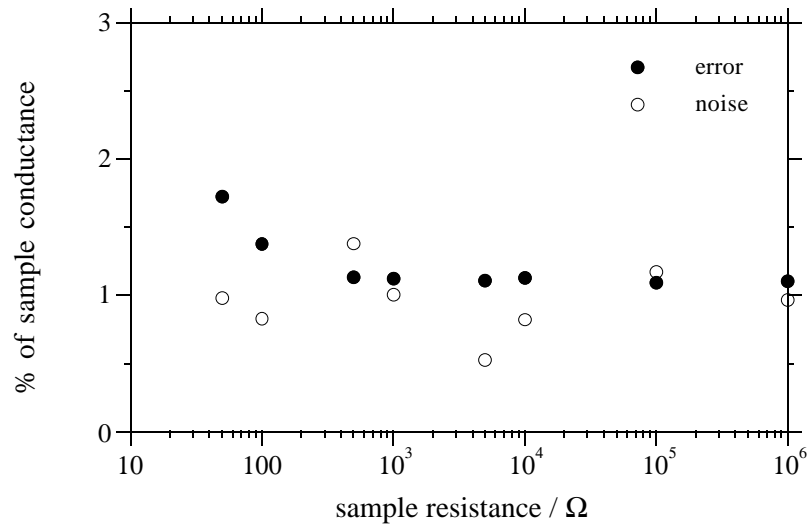


**Fig. 5.6.** Error and noise in the numerically calculated conductance of known resistances. Each conductance was calculated from an  $I$ - $V$  sweep of 101 points over  $\pm 100$  mV.

## 5.2.2 Numerical Differentiation and Smoothing

A numerical differentiation routine, derived from Stirling's interpolation formula, was used to calculate the dynamic conductance from the measured  $I$ - $V$  curves (Hosking *et al.* 1986). If  $f_m = f(x_m)$  is a function tabulated at points  $x_0, x_1, \dots, x_N$ , which are evenly spaced with separation  $h$ , then the derivative is approximately

$$f'(x_m) = \frac{1}{h} \sum_{k=0}^{\infty} \left( \frac{(-1)^k (k!)^2}{(2k+1)!} \mu \delta^{2k+1} f_m \right) \quad (5.7)$$

where, for odd  $r$

$$\mu \delta^r f_m = \frac{1}{2} \sum_{j=0}^{(r+1)/2-1} (-1)^j \left( {}^r C_j - {}^r C_{j-1} \right) \epsilon_{(r+1)/2-j} f_m$$

$${}^r C_j = \begin{cases} \frac{r!}{j!(r-j)!} & j \geq 0 \\ 0 & j < 0 \end{cases}$$

and the 'range difference operator' is defined as  $\epsilon_r f_m = f_{m+r} - f_{m-r}$ . If just the first term of (5.7) is used then

$$f'(x_m) = \frac{1}{2h} \epsilon_1 f_m = \frac{1}{2h} (f_{m+1} - f_{m-1})$$

This is the familiar central difference expression, which only uses nearest-neighbour tabulated points. Retaining two terms in (5.7) uses the nearest two neighbouring points from each side, etc.

One might expect that use of  $f(x_{m\pm 3})$  to calculate  $f'(x_m)$  would lead to excessive broadening in the derivative; however, testing the routine on dummy data showed that using higher terms in (5.7) results in greater accuracy. The increased accuracy is rapidly lost however, as noise is introduced into the data; if noise is greater than 1% no advantage is gained from using more than one term.

Numerically calculated conductance-voltage curves of point-contact junctions were frequently very noisy, with the level of noise increasing with bias voltage. The noise was much larger than observed in resistors with the same value and is attributed mainly to vibrational disturbance of the delicate contact. Consider an ohmic contact with a voltage-independent fluctuating conductance,  $G \pm \Delta G$ . If this conductance is found by numerical differentiation of a measured  $I$ - $V$  curve then the observed noise is

$$\delta G(V) \approx \frac{V}{h} \Delta G$$

This expression shows that the d.c. measurement technique is intrinsically more noisy than a direct measurement of conductance, since  $V/h \gg 1$ , and that attempts to increase voltage resolution by decreasing  $h$  will further increase the noise.

An alternative source of noise was discussed by Cockburn (1988). He observed that noise in the conductance of point-contact tunnel junctions did not increase uniformly but rose rapidly above a threshold voltage of about 100 mV. This phenomenon was attributed to fluctuation in tunnelling barrier height due to changes in the electronic population of defect or impurity states in the barrier. This effect has been seen in many small-area tunnelling systems and so probably contributes to the noise observed in the present study. Indeed, some point contacts did show a dramatic increase in noise above a particular threshold voltage (figure 5.7).

Some useful information might still be present in noisy conductance–voltage characteristics, since fitting a model to the data is perfectly legitimate if errors are used correctly. A numerical routine may be used to construct a smoothed curve, which helps with selection of data sets that are suitable for fitting. This curve should simply serve to guide the eye through the scattered raw data points, each with a large error bar, and should always be presented together with the original data.

The simplest smoothing routine is an unweighted average of the nearest neighbouring points. The data is listed in order of increasing abscissa value ( $x_0, x_1, x_2, \dots$ ) and the ordinates of the nearest  $r$  data points on either side of  $x_m$  are averaged to give the smoothed value, i.e.,

$$\bar{f}(x_m) = \frac{1}{2r+1} \sum_{j=0}^{+2r} f(x_{m-r+j})$$

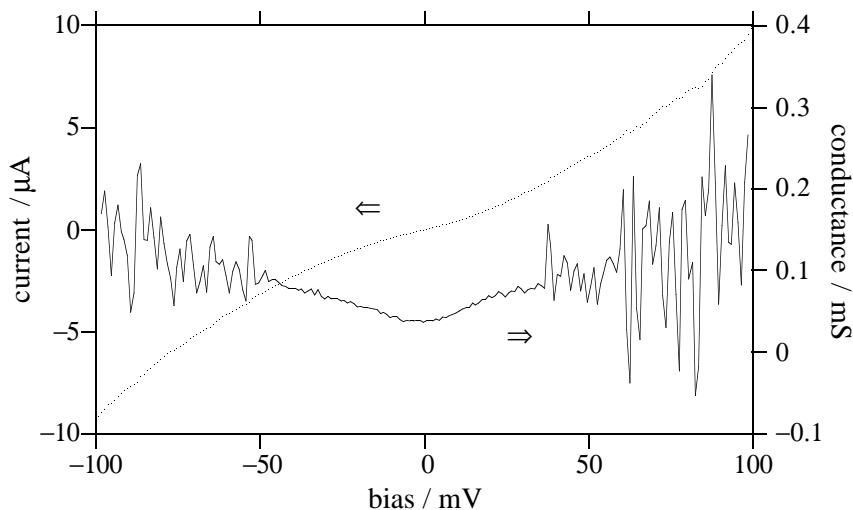


**Fig. 5.7.** Characteristics of a  $W \rightarrow (\text{Tl,Pb})(\text{Ca,Ce})\text{Sr}_2\text{Cu}_2\text{O}_y$  point-contact.

CHAPTER 5 117

The width of the averaging window,  $2r+1$ , sets the level of smoothing. This method is particularly suited to smoothing of data with an error distribution that has a broad tail (Press *et al.* 1987).

Several other smoothing routines were tried including low-pass filtering of a fast fourier transform (FFT) of the raw data and ‘windowed averaging’ with various weighting functions over the window width. It was hoped that these would smooth the data equally well but with reduced broadening of sharp features. However, neither of these significantly improved upon smoothing by the unweighted averaging method. In addition there was some evidence that peak-like structure was left in the smoothed data as an artefact of the FFT procedure.

The standard numerical analysis procedure employed throughout this work was to differentiate using three terms in Stirling’s numerical expression (5.7) and then smooth with an unweighted ‘window’ of width five (i.e.,  $r = 2$ )\*. The analysis was performed by a program which batch processed all files stored in a specified directory and automatically produced conductance–voltage plots. This allowed a large number of current-voltage curves to be analysed rapidly and in a consistent manner.

Some signal averaging was available at the time of data acquisition to reduce noise in the measured  $I$ – $V$  characteristics. The CIL6580 unit contained a digital filter which could be programmed to return the average of  $2^n$  ADC readings ( $n = 0$ – $15$ ). This was carried out rapidly by the CIL6580’s hardware each time a data acquisition was requested and required no further communication with the controlling computer. In this way each point of the  $I$ – $V$  curve was averaged as it was collected.

Averaging could also be carried out by combining complete  $I$ – $V$  curves. To indicate any changes in the characteristics the set of points from the most recent voltage sweep was displayed together with a rolling average of all curves taken since initiating the acquisition. After each sweep the user was asked whether to add the new data to the rolling average and initiate another sweep, or ignore it and abort the acquisition process. This choice was assisted by the program, which warned if any point in the new data set differed from the rolling average by more than a pre-set amount. The program could also be configured to test the new data set automatically, include it in the rolling average if every point was valid and trigger the next voltage sweep. Acquisition was stopped automatically when any point in the new set was too far from the rolling average.

---

\* As pointed out by Speakman (1993), if the first term in (5.7) dominates then this procedure actually loses all information from points  $f_m$ ,  $f_{m-1}$  and  $f_{m+1}$  !

### 5.2.3 Additional Features of the D.C. Measurement System.

The CIL6580 and control program may be used to simultaneously measure the current, conductance and capacitance of a sample. The latter two quantities are read, via additional ADCs, from the in-phase and quadrature outputs of a lock-in amplifier set up as shown in figure 5.1. Linear calibration models enable these readings to be stored as accurately calibrated voltages. Alternatively, by entering the lock-in sensitivity and the modulation amplitude and frequency, the conductance and capacitance values are calculated immediately. Figure 5.8 is an example of data taken in this way. It also compares conductance–voltage characteristics obtained by the a.c. and d.c. methods.

The program may be configured to make multiple voltage sweeps - either averaging the readings (as described above) or storing them individually - and then to wait for a pre-defined period of time before making another set of sweeps. During this waiting period the CIL6580 outputs an adjustable d.c. voltage. The program may also be set to start a new sweep immediately or wait until prompted by the user to continue. These facilities have recently been used to investigate time- and voltage-dependent annealing effects in MIM tunnel junctions (Holden 1992).

### 5.2.4 Possible Improvements to the D.C. Measurement System

The d.c. measurement system is too slow. Measurement, processing and plotting of a single current–voltage point took 45 ms, of which 16 ms was spent communicating data between the CIL6580 unit and the computer via the serial RS-232 interface (at 9600 baud). Communication time could have been reduced to less than 0.5 ms by

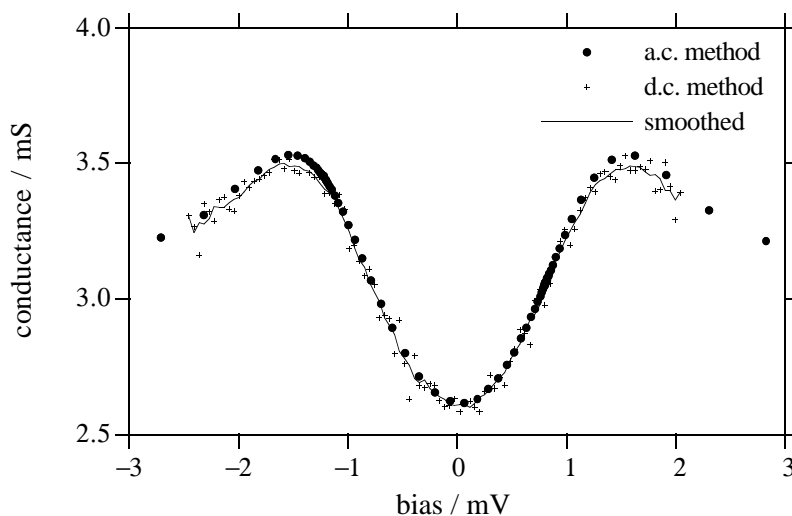


**Fig. 5.8.** Comparison of conductance–voltage characteristics measured by the a.c. modulation technique (single sweep) and by numerical differentiation of the average of 382  $I$ – $V$  sweeps. The sample is an evaporated Pb/Al–Al<sub>2</sub>O<sub>3</sub>–Al proximity-effect junction.

using a parallel IEEE-488 interface; however, this required additional hardware which was unavailable. A further 18 ms could be gained simply by using a faster host computer.

The computer program that controls the CIL6580 unit operates in a local way. For each measured point on the  $I$ - $V$  curve an 'output voltage' command must be sent to the CIL6580 from the computer. The computer then delays before sending a 'trigger ADC' command which prompts the unit to read a voltage and send the resulting number back to the Macintosh. It should be possible to run this simple source-sense cycle from a program written with the CIL6580's built-in programming language. A table of output voltages would be pre-defined in the unit's RAM together with controlling code. On receiving a single 'trigger acquisition' command the internal program would be executed and data would be collected from the appropriate ADCs and stored in the unit's own memory. After collecting data from a complete voltage sweep the whole set of points could be transmitted to the computer. It is difficult to estimate the speed advantage that would be gained by operating the CIL6580 unit in this remote way. A pseudo-parallel-processing arrangement could possibly be used, with the host computer analysing previous data sweeps whilst the CIL6580 unit collected a new set. In addition, overheads due to communication of small chunks of data would be avoided.

Preliminary investigations indicate that the simplicity of the CIL6580's internal language would make this a formidable programming problem. Difficulties are envisaged with attempts at synchronising the two programs and hardware handshaking would probably be required. Documentation of the CIL6580's hardware and software is extremely poor and the manufacturer is reluctant to answer technical enquiries.

Rather less fundamental changes could be made to the program currently used. The program is only able to calibrate the output of a lock-in amplifier positioned in the circuit as shown in figure 5.1. An option to calibrate a lock-in placed across the arms of the bridge circuit would also be useful and would be a simple modification. The original intention was to read voltages from only one ADC. Routines to read an additional two channels were 'tacked on' rather than logically integrated into the code. It should be possible to write a more general data-logging program that is able to use all eight ADCs and four DACs and that can apply a general calibration procedure to each channel. One way of doing this would be to use a higher-level programming language, such as LabView\*, which is specifically designed to simplify computer interfacing.

---

\* Manufactured by National Instruments, Newbury, Berkshire.